ResearchGate

See discussions, stats, and author profiles for this publication at: https://www.researchgate.net/publication/231709843

The Role of Co-Units in Polymer Crystallization and Melting: New Insights from Studies on Syndiotactic Poly(propene-co-octene)

ARTICLE *in* MACROMOLECULES · AUGUST 1998

Impact Factor: 5.8 · DOI: 10.1021/ma980453c

CITATIONS
105

READS
11

3 AUTHORS, INCLUDING:

Juergen Schmidtke
Universität Paderborn
21 PUBLICATIONS **800** CITATIONS

SEE PROFILE

Available from: Juergen Schmidtke
Retrieved on: 26 January 2016

The Role of Co-Units in Polymer Crystallization and Melting: New Insights from Studies on Syndiotactic Poly(propene-*co*-octene)

G. Hauser, J. Schmidtke, and G. Strobl*

Fakultät für Physik, Albert-Ludwigs-Universität, 79104 Freiburg, Germany

Received March 23, 1998; Revised Manuscript Received June 8, 1998

ABSTRACT: The effect of noncrystallizable units on the crystallization and melting was studied for two octene copolymers of syndiotactic polypropylene, in an extension of previous investigations on a homopolymer sample with 3% meso diads. Using time and temperature dependent SAXS experiments and DSC, we determined the dependencies of the crystal thickness, the rate of crystallization, and the melting point on the chosen crystallization temperature. With an increase in the content of noncrystallizable units (octene units or meso diads; both show equal effects), we observed, as expected, a shift of the melting points to lower temperatures and similar shifts of the growth rate versus temperature curves, but surprisingly, no effect at all on the crystal thickness. The thicknesses of all three samples show a common temperature dependence, being inversely proportional to the supercooling below the equilibrium melting point of perfect syndiotactic polypropylene. The latter is located at 196 °C, as determined by an extrapolation based on measured melting points. Data demonstrate that the popular Hoffman−Weeks plot when applied to random copolymers does not yield the respective equilibrium melting points; it can only be used for perfect homopolymers. Crystal thicknesses and growth rates are, according to the observations, independent properties. The thicknesses are those of a specific native crystal form with high surface free energy. DSC experiments indicate that all crystals first form this native state and then become stabilized by relaxation processes that decrease the surface energy. These stabilization processes, which produce the difference between the temperatures of crystallization and melting, leave the crystallite thickness unchanged.

1. Introduction

The introduction of co-units at random positions of a chain generally leads to a downward shift of the temperature ranges of crystallization and melting accompanied by a decrease of the crystallinity. The effect is qualitative, as expected, comparable to the melting point depression in low molecular weight compounds resulting from the addition of a noncrystallizable solute to the melt. Quantitative treatments of the effect, however, are rare, not only due to a lack of satisfactory theoretical approaches but also because of a lack of experimental data having the completeness necessary for a detailed analysis. In usual works DSC experiments are carried out to find the melting point and its change with the crystallization temperature. Then the linear Hoffman−Weeks extrapolation[1] is used to determine the temperature where the difference between the crystallization and the melting temperature apparently vanishes. This point is understood as representing the equilibrium melting point of the copolymer. If samples with different co-unit contents are available, data are commonly evaluated by employing Flory's copolymer equation,[2] usually in its simplest form, which relates the melting point depression to the heat of melting and the content of co-units only (ref 3 is one example). As a matter of fact, looking through the literature, one rarely finds agreement between Flory's theoretical prediction and measured data. In the majority of cases shifts are much larger than expected.

Clearly, the main shortcoming of this kind of investigations is the complete lack of structural data. Indeed, the melting point of a polymer crystallite depends on both its thickness and the content of co-units. One might also expect, at first, that the thickness of the crystallites formed at a given crystallization temperature would change with the co-unit fraction. Therefore, to really extract the effect of the co-units, a knowledge of the crystallite thickness is definitely required.

Recently, we carried out a comprehensive study on the crystallization and melting behavior of syndiotactic polyproylene.[4] Using both calorimetry and small-angle X-ray scattering we could accurately determine the dependence of the crystal thickness and the melting point on the chosen crystallization temperature. This was possible because time and temperature-dependent SAXS experiments showed that crystals of s-PP keep their thickness constant, both during the isothermal crystallization process and a subsequent heating to the melting point. As a first clear result, data demonstrated that the Hoffman−Weeks procedure can be incorrect. The point where the difference between the crystallization and the melting point apparently vanishes is here associated with a finite crystal thickness and located below the true equilibrium melting point.

In spite of their uniform thickness s-PP crystallites greatly vary in stability. Melting starts shortly above the crystallization temperature and then the rate increases and reaches a maximum near the end of the melting range. We understand the observations as indicating that the crystallization from the melt takes place in two steps. The first step is the formation of imperfect "native crystallites" and it is followed by structural relaxation processes transferring them into the final form. The relaxation processes leave the thickness unchanged and may concern both the surface and the interior. The majority of the crystallites reach the highest possible perfection; i.e. they remain stable up to the final melting point. For others, the relaxation remains incomplete and they melt earlier. After their

* To whom correspondence should be addressed.

S0024-9297(98)00453-7 CCC: $15.00 © 1998 American Chemical Society
Published on Web 08/15/1998

melting, crystallites may form again, with an increased thickness. Analysis of this "melting−recrystallization process" showed that the recrystallization takes place with much higher rates than the primary crystallization, which suggests persistence of a partially disentangled melt state. The observations led us to the statement that in discussions of the crystallization and melting behavior of polymers it might be appropriate to use a "four-state scheme", with two states for the melt, the original entangled state, and a temporary state established immediately after the melting, as well as two states for the crystallites, the initial imperfect form and the final equilibrated state reached at the end.

We were aware that the syndiotactic polypropylene under study was not perfect, as it included 3% meso diads. Melting and crystallization certainly were affected by their presence. Therefore we found it necessary and worthwhile to further extend the studies and to investigate some more statistical copolymers. We were happy to obtain appropriate samples from the neighboring Institute of Macromolecular Chemistry, copolymers which included octene units in two different contents, 1.7 and 6.4 mol %. For these compounds we carried out the same experiments as for the s-PP sample; i.e., we determined growth rates and crystal thicknesses for different crystallization temperatures and analyzed the subsequent melting. This paper reports on the results. Some of them were unexpected and are truly surprising. They appear important, not only for the understanding of the co-unit effect but also for our understanding of polymer crystallization and melting in general.

2. Experimental Section

2.1. Instrumentation. Differential scanning calorimetry was carried out using a Perkin-Elmer DSC 4. The kinetics of isothermal crystallization was monitored in time dependent runs; the melting behavior was studied by heating samples with various rates in the range 1−10 K min^{-1}. SAXS experiments were conducted with the aid of a Kratky camera attached to a conventional X-ray source, which is equipped with a temperature-controlled sample holder. The changes of the structure during isothermal crystallization and the melting on heating were followed by measuring the scattering curves with a position sensitive metal wire detector. A few minutes counting time were sufficient for a curve registration. Deconvolution of the slit-smeared data was achieved by applying an algorithm developed in our group.[5] Analysis was based on the one-dimensional correlation function $K(z)$ and its second derivative $K''(z)$. Both follow from the SAXS data by carrying out appropriate Fourier transformations. The main properties of interest are the thickness of the crystalline lamellae d_c (crystalline core plus half of the transition zones on both sides, compare ref 6, p 412) and the specific internal surface O_{ac} (the interface per unit volume separating crystalline and amorphous regions). All details of the procedure applied to derive these properties from $K(z)$ and/or $K''(z)$ have been given previously.[4] In this paper we display for demonstration only a few of the curves $K''(z)$ measured during time and temperature dependent experiments. For an understanding it is sufficient to know that these curves directly reflect the thickness distribution of the crystallites.[7] The location of the peak of $K''(z)$ yields the (most probable) crystal thickness d_c. Some of the curves are expressed in terms of the Porod coefficient $P \sim (\Delta\eta)^2 O_{ac}$ ($\Delta\eta$: electron density difference between the crystalline and amorphous regions).

Table 1. Properties of s-Polypropylene and s-Poly(propene-*co*-octene) Samples

sample	octene units % (weight)	octene units % (mole)	% meso diads	M_n	M_w/M_n
s-PP	0	0	3	104 000	1.7
s-P(P-*co*-0)4	4	1.7	(3)	73 000	2.1
s-P(P-*co*-0)15	15	6.4	(3)	94 000	1.7

2.2. Samples. The experiments were carried out on two samples of syndiotactic poly(propene-*co*-octene). They were synthesized by S. Jüngling in the Institute of Macromolecular Chemistry of our university using a metallocene catalyst. Details are described in ref 8. The chemical properties of the two samples are given in Table 1, together with those of the

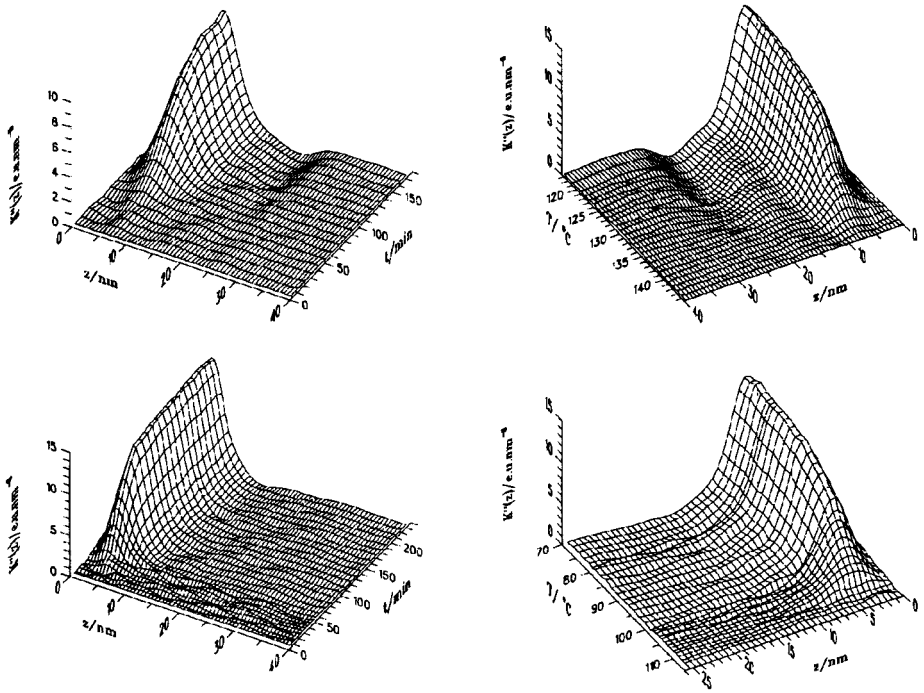

Figure 1. Functions $K''(z)$ giving the distribution of crystal thicknesses, obtained by time and temperature dependent SAXS experiments: Changes during isothermal crystallization of s-P(P-*co*-O)4 at 116 °C (top left) and of s-P(P-*co*-O)15 at 70 °C (bottom left) and during the subsequent melting processes (right-hand sides).

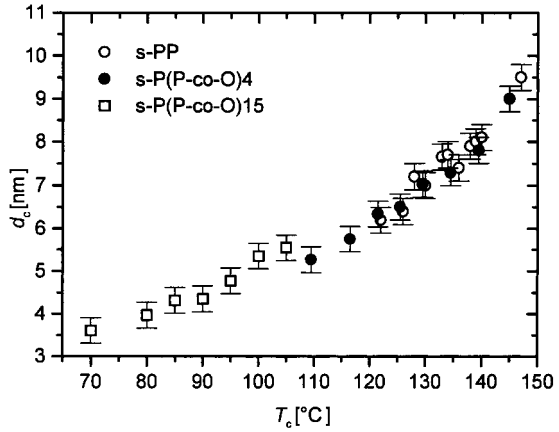

Figure 2. T_c dependence of the crystal thickness of the different samples.

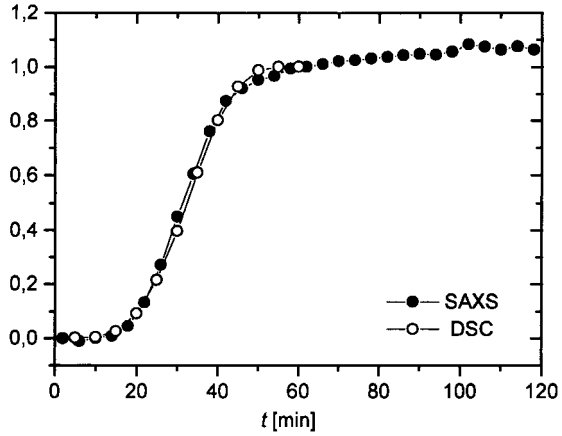

Figure 3. Kinetics of isothermal crystallization of s−P(P-*co*-O)4 at 109.5 °C, as observed in time dependent SAXS and DSC measurements, respectively.

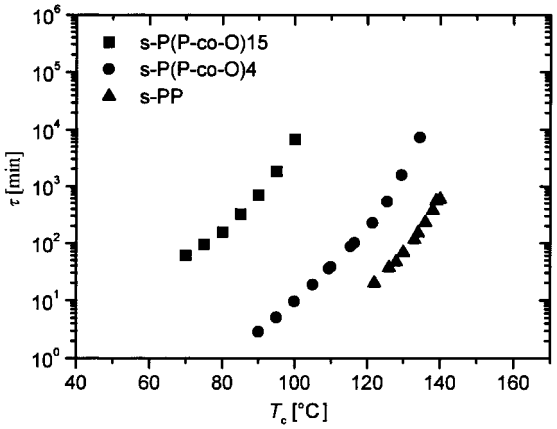

Figure 4. Avrami times of crystallization dependent on the crystallization temperature.

s-PP sample investigated previously. Co-unit contents were determined by NMR spectroscopy. A determination of the fraction of meso diads included in the octene copolymers was not possible due to an overlap of the signals. However, as the polymerization conditions were the same as those for the s-PP sample, no change in the stereoregularity is expected. Indeed, the experimental results presented later support this view. Considering the size of the side groups associated with the octene units, their incorporation into the crystallites appears highly improbable. A complete exclusion is also expected for the meso bonds since they destroy the helical structure. Measured WAXS diagrams[9] confirm this expectation: Position and width of the main crystal reflections do not change between the three samples. In addition, for s-PP and s-P(P-*co*-O)4 the 211 reflection indicative for a perfectly ordered lattice with two right- and two left-handed helices passing through a unit cell[10] is observed. For s-P(P-*co*-O)15 the 221 peak did not appear; i.e., a long-ranged antichiral packing was not achieved.

3. Results

3.1. SAXS Determination of Crystal Thicknesses. The crystallite formation during isothermal crystallization was studied in time dependent SAXS experiments in the same way as previously for s-PP. The temperature ranges covered were 110−145 °C for s-P(P-*co*-O)4 and 70−105 °C for s-P(P-*co*-O)15. After the isothermal crystallization the melting was monitored in temperature dependent SAXS measurements up to the melting point. Data evaluation was based on the one-dimensional correlation function $K(z)$ and its second derivative $K''(z)$ derived from the scattering data. Figure 1 displays as an example the curves $K''(z)$ for s-P(P-*co*-O)4 during and after an isothermal crystallization at 116 °C and for s-P(P-*co*-O)15 during and after an isothermal crystallization at 70 °C. The formation and melting of the crystallites shows up in the changing height of the ridge dominating $K''(z)$. The location of the ridge gives the crystal thickness. As was already observed for s-PP, this thickness remains constant through both the time of isothermal crystallization and the subsequent melting. Curves indicate thicknesses of 5.7 and 3.5 nm for the s-P(P-*co*-O)4 and s-P(P-*co*-O)-15, respectively. Observations were similar for all other chosen crystallization temperatures. As a result of all measurements, we obtained for the two copolymers the dependencies of the crystallite thickness on the crystallization temperature, denoted T_c. These are displayed in Figure 2 together with the previous results obtained for s-PP. The outcome is most surprising: As it appears, we have a common dependence for all samples; i.e., d_c does not depend on the content of co-units but only on the crystallization temperature. According to a common view, crystal thicknesses should depend on the supercooling below the respective equilibrium melting point, which changes with the co-unit content. Our observations contradict this assumption.

3.2. Rates of Crystallization. Growth rates for the process of isothermal crystallization were deduced from both time dependent SAXS experiments and conventional calorimetry. The SAXS measurements were used for the higher crystallization temperatures; DSC measurements, in the range of lower temperatures. A comparison was possible in a restricted overlap region. As demonstrated by the curves in Figure 3, we find perfect agreement. Kinetic curves may be satisfactorily represented by the Avrami expression $1 - \exp[-(t/\tau)^{\beta}]$ with exponents in the range $\beta = 3-4$. We used τ as the characteristic crystallization time. Figure 4 shows the values obtained by DSC and SAXS for the copolymers and the s-PP. The effect of the co-units on the crystallization rate is quite strong. At a fixed crystallization temperature one observes an increase in τ by 1 order of magnitude between s-PP and s-P(P-*co*-O)4 and by 3 orders of magnitude between s-P(P-*co*-O)4 and s-P(P-*co*-O)15. It appears that all the curves $\tau(T_c)$ have a similar shape, being just shifted along the temperature axis.

Crystallinities reached at the end of isothermal crystallization decreased, as expected, from s-PP to s-P(P-*co*-O)4 to s-P(P-*co*-O)15. Typical values were 29%

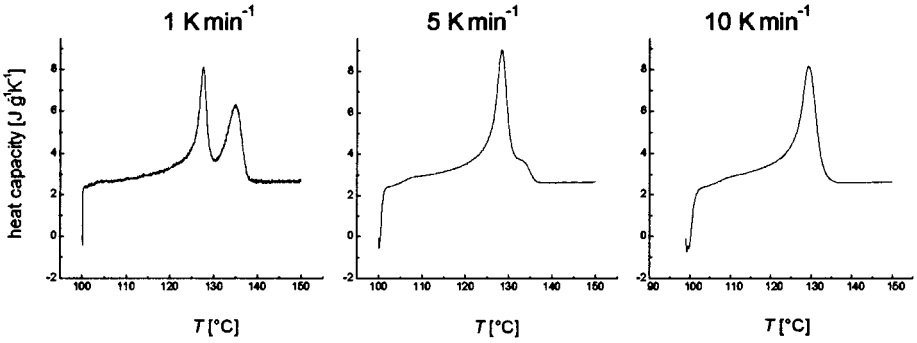

Figure 5. s-P(P-*co*-O)4, crystallized at 100 °C. DSC melting curves measured using the indicated heating rates.

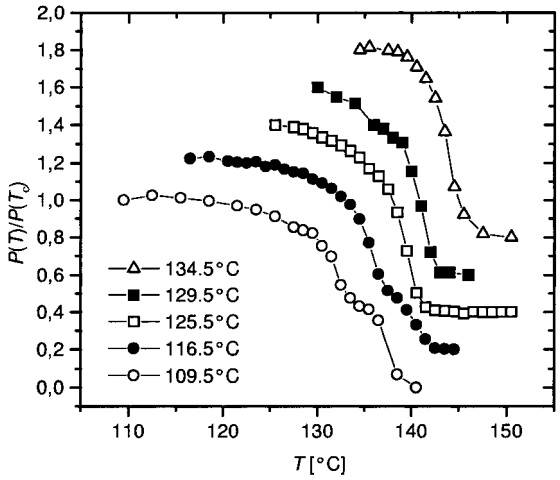

Figure 6. Melting of s−P(P-*co*-O)4 after an isothermal crystallization at the indicated temperatures, followed by the changes of the Porod coefficient. Curves are vertically shifted by steps of 0.2 units.

for s-PP, 20% for s-P(P-*co*-O)4, and 14% for s-P(P-*co*-O)15, obtained for Avrami times on the order of hours.

3.3. Melting Behavior. For s-PP we had clear evidence for a recrystallization after melting. The same effect is observed for the copolymers. Figure 5 shows as an example the melting behavior of s-P(P-*co*-O)4 after an isothermal crystallization at 100 °C. A second peak shows up after the melting, and its weight decreases with increasing heating rate, which is indicative for a recrystallization process. As was already found for s-PP, the effect is pronounced for low crystallization temperatures or low heating rates and becomes diminished and finally disappears when going to higher crystallization temperatures and heating rates. The melting−recrystallization process can also be observed in the SAXS experiments. Figure 6 collects some results that were again obtained for s-P(P-*co*-O)4. For T_c = 109.5 °C one observes a two-step decay in the scattering intensity. At the higher crystallization temperature the effect disappears. Results of differential scanning calorimetry and SAXS are in agreement, as is demonstrated by Figure 7. Curves refer to the melting of s-P(P-*co*-O)15 after a crystallization at 70 °C, both being registered with the same heating rate.

Clearly, when asking for the value of the melting point of the crystallites, T_f, one has to choose the first DSC peak or the location of the first decay in the temperature dependent SAXS curve. Figure 8 collects all values T_f thus obtained. The dependencies T_f (T_c) found for s-PP and the two copolymers are given using filled symbols. Data for each sample fall on one line

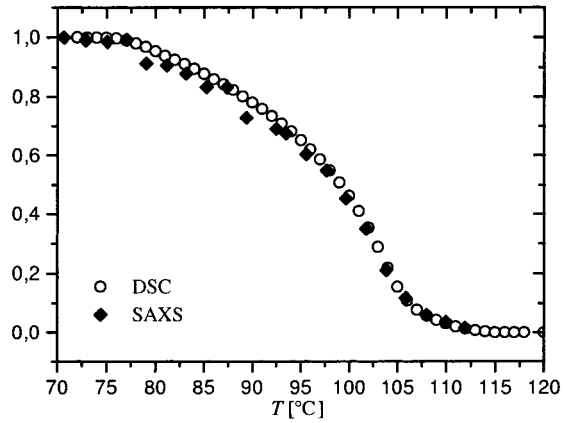

Figure 7. Melting of s−P(P-*co*-O)15 after an isothermal crystallization at 70 °C. Comparison of DSC and SAXS data obtained with the same heating rate (1 K min^{-1}).

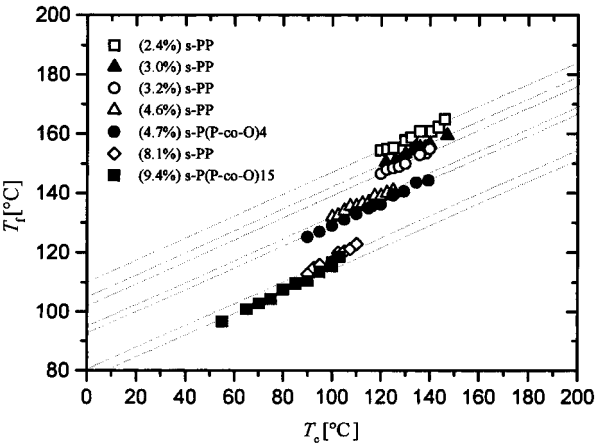

Figure 8. Temperature of the melting peak dependent on T_c. Results of this work are given using filled symbols. Also included are data of Balbontin et al. (open symbols).

and all lines have the same slope. As expected, melting points decrease with increasing co-unit content.

The melting point T_f just represents the temperature with the maximum melting rate. Indeed, as was already pointed out in the discussion of the melting behavior of s-PP, melting extends continuously from the crystallization temperature T_c to T_f. This becomes even more clear when looking at the experiments on the copolymers. Figure 9 collects melting curves measured for s-P(P-*co*-O)15 after isothermal crystallizations at three different T_c's. In all these cases crystallization was not continued up to the end but stopped after different times, thus allowing the observation of changes. For short crystallization times melting sets in smoothly, but for longer times a different behavior appears. A

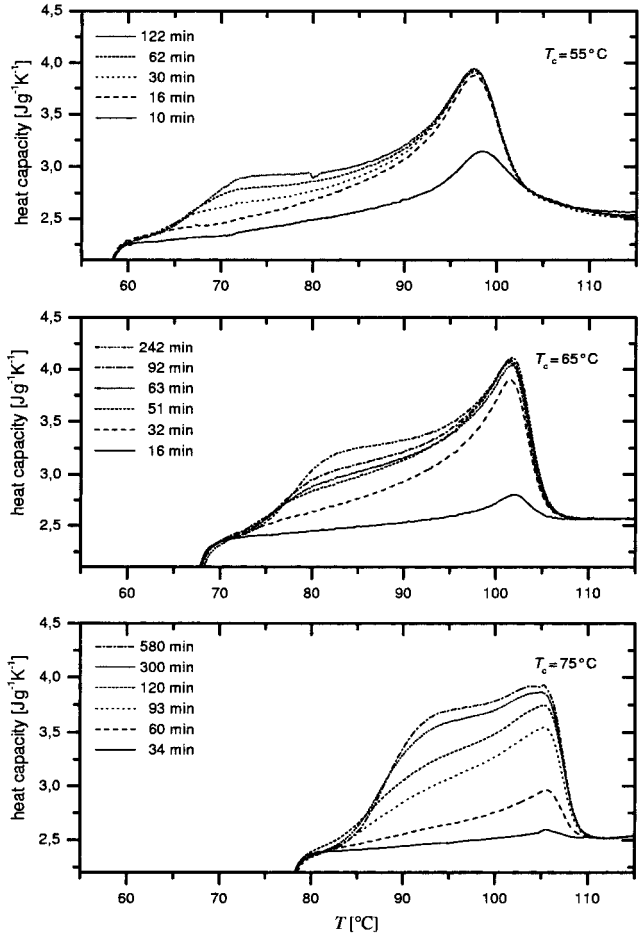

Figure 9. s-P(P-*co*-O)15: DSC melting curves obtained after different times of isothermal crystallization at 55 °C (top), 65 °C (center), and 75 °C (bottom).

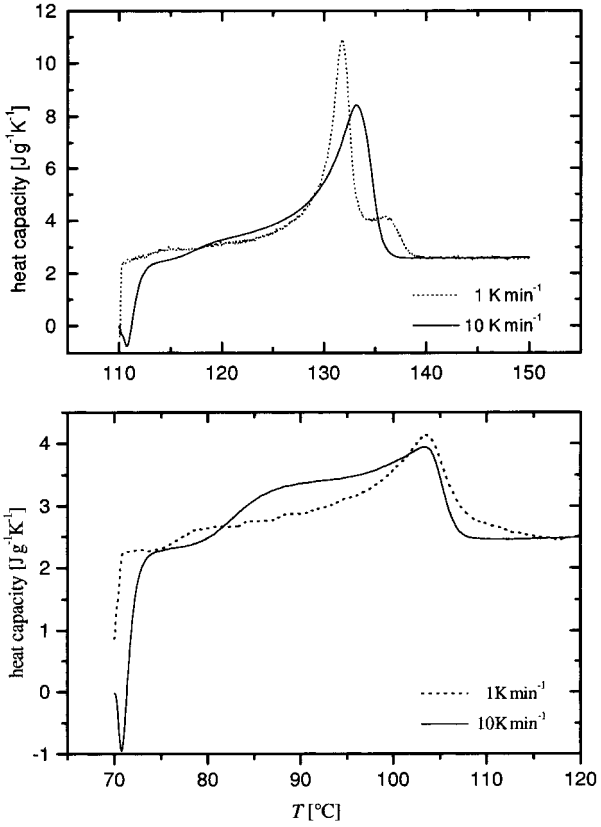

Figure 10. s-P(P-*co*-O)15, isothermally crystallized at 70 °C: Change of the melting curve with the heating rate (bottom). Analogous experiment for s-P(P-*co*-O)4 crystallized at 110 °C (top).

second contribution evolves in the diagram on the low-temperature side, indicative of the existence of crystallites with lower stability. For the long crystallization times these even build up a second peak. Melting always starts about 5 °C above T_c with an uprise, leading to a maximum after additional 8 °C. Note that the weight of this second component increases with the crystallization time. This weight, however, is not fixed. As demonstrated by the measurements shown in Figure 10, it changes with the heating rate. In fact, the lower the heating rate, the smaller is the contribution of the low-temperature peak. Obviously, crystals perfect if sufficient time is provided during the heating. Figure 10 shows measurements on both copolymers, s-P(P-*co*-O)4 and s-P(P-*co*-O)15. The effect is less pronounced for s-P(P-*co*-O)4 but certainly also present.

4. Combined Effect of Thickness and Co-Units on T_f

Flory's widely used equation describing the equilibrium melting point of a random copolymer in the case of perfect exclusion of the co-units from the crystal lattice reads[2]

$$T_f^{\infty,0} - T_f^{\infty}(x_B) = \frac{k(T_f^{\infty,0})^2}{\Delta h} x_B \qquad (1)$$

The depression of the melting points with regard to the homopolymer is proportional to the fraction of noncrystallizable units x_B and inversily proportional to the heat of melting per monomer Δh (k is the Boltzmann constant; we write $T_f^{\infty,0}$ for the equilibrium melting point of the homopolymer). Flory's equation is identical to Raoult's law of the melting point depression in low molar mass systems following from the addition of an athermal noncrystallizable solute. As was already pointed out, measured melting points are always affected by both x_B and d_c. We have separated in our experiments the two dependencies and therefore first write down an equation which accounts for both factors.

In the derivation we proceed, somewhat intuitively, as follows. Consider a growing polymer crystallite with a lateral growth face of area a. Before it can grow further by a step Δx all co-units in front of the growth face within a volume $a\Delta x$ have to be removed. This implies a work

$$\Delta W = \rho_{osm} a \Delta x \qquad (2)$$

against the osmotic pressure exerted by them. As Flory did, we assume perfect conditions where

$$p_{osm} = \rho_B kT \qquad (3)$$

ρ_B giving the number density of the co-units randomly distributed along the chains. Then the work follows as

$$\Delta W = kTN_B \qquad (4)$$

where N_B denotes the number of co-units within the volume $a\Delta x$. Crystallization is associated with a decrease in the Gibbs free enthalpy. If the stems building up the crystallites are composed of n monomers, a transfer of N_A monomers into the crystalline state leads

to a gain in the Gibbs free enthalpy of

$$\Delta G_c = -N_A\left(g^a - g^c - \frac{2\sigma_e}{n}\right) \quad (5)$$

Here, g^a and g^c denote the chemical potentials (per monomer) in the melt and the crystal respectively; the last term proportional to the inverse of n accounts for the effects of the two crystal surfaces, σ_e describing the surface tension per end group (to be understood as including also the Gibbs free enthalpy increases of the monomers in the transition region). Clearly crystallization can only proceed if the total change of the Gibbs free enthalpy

$$\Delta G = \Delta W + \Delta G_c \quad (6)$$

remains negative. This change is

$$\Delta G = kTN_B - N_A\left(g^a - g^c - \frac{2\sigma_e}{n}\right) \quad (7)$$

For $\Delta G = 0$ we are at the equilibrium melting point of the crystallites. This occurs for

$$g^a - g^c = kT\frac{N_B}{N_A} + \frac{2\sigma_e}{n} = kTx_B + \frac{2\sigma_e}{n} \quad (8)$$

(using $x_B = N_B/(N_A + N_B) \approx N_B/N_A$). Applying the series expansion

$$(g^a - g^c)(T) \approx \frac{\Delta h}{T_f^{\infty,0}}(T_f^{\infty,0} - T) \quad (9)$$

we finally obtain

$$T_f^{\infty,0} - T_f(x_B, n) \approx \frac{k(T_f^{\infty,0})^2}{\Delta h}x_B + \frac{2\sigma_e T_f^{\infty,0}}{\Delta h}\frac{1}{n} \quad (10)$$

As we see, the effects expressed by Raoult's law and by the Gibbs−Thomson equation are just superposed.

5. Discussion

5.1. Comparison with the Data of Balbontin et al. Using DSC, Balbontin et al. investigated a series of syndiotactic polypropylenes with various contents of meso diads, obtaining for all samples the relations between the melting temperature and the temperature of crystallization.[3] It is interesting to compare their data with our results, and they are included in Figure 8 using open symbols. Balbontin's data also show a linear dependence between T_f and T_c and we find the same constant slope. The order of the lines is systematic, considering that the relevant parameter is the sum of the fraction of meso diads and the fraction of octene units, which represents the total fraction of noncrystallizable units (the values are given in the drawing). Shifts exactly follow these numbers: The higher the fraction x_B of noncrystallizable units, the lower are the melting points. Figure 11 displays this dependence for a fixed $T_c = 100$ °C, whereby the melting points were determined either by direct measurements or by the linear laws. The data of Balbontin and us show a common dependence on x_B. Obviously, the units at a meso bond are also excluded from the lattice and they introduce, therefore, the same effect as the octene units. We find for $x_B < 5\%$ a linear change of T_f; at higher values of x_B there occurs a change in the slope, commonly for both kinds of samples.

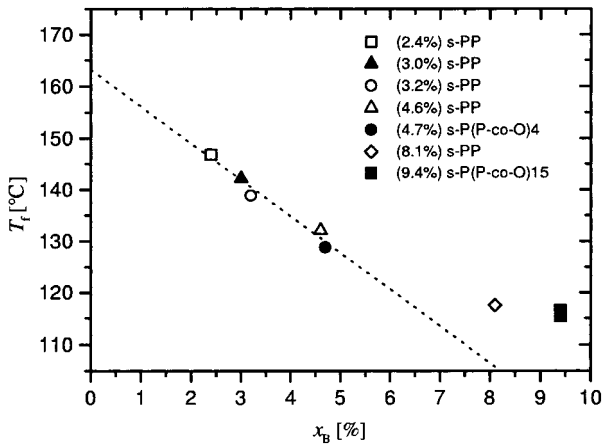

Figure 11. Melting peak temperatures T_f of samples with different contents of noncrystallizable units (meso diads and octene units) for a constant crystallization temperature of 100 °C.

Regarding the equal roles of meso diads and octene units, the observation of a constant crystallite thickness of s-PP throughout the isothermal crystallization and a heating to the melting point is no longer surprising: The presence of the meso diads prevents all solid-state thickening processes. Growth of a crystal requires a selection of syndiotactic sequences with lengths above d_c. For a random distribution of the noncrystallizable units these sequences exist for any given d_c, with decreasing number on increasing x_B. Crystallization results in a transfer of the too short sequences into the interlamellar amorphous regions. The separation leads also to an accumulation of the noncrystallizable units at the crystallite surfaces, which block the solid-state thickening and fix the crystal thickness.

5.2. Equilibrium Melting Point of Perfect s-PP. We are now in the position to determine the equilibrium melting point of perfect s-PP. First, by combination of the data shown in Figures 2 and 8 we establish the relation between d_c and T_f. As suggested by the Gibbs−Thomson equation, we present this dependence in the form $d_c^{-1}(T_f)$. As shown by Figure 12 straight lines are indeed obtained.

To obtain the equilibrium melting point of perfect s-PP, two effects have to be added, first the melting point reduction following from the fraction of noncrystallizable units, keeping the crystal thickness constant, and second the reduction due to the finite crystal thickness, keeping x_B constant. Referring to the s-PP sample, Figure 11 indicates a melting point reduction of 20 K due to x_B. If we add this value to the equilibrium melting point of this sample, which follows from Figure 12 as 176 °C, we obtain for the equilibrium melting point of a perfect s-PP, the value 196 °C. The result can be used to give the Gibbs−Thomson line expected for a perfect s-PP. It starts from the equilibrium melting point having the same slope as all samples. The dashed line in Figure 12 shows this extrapolated dependence.

Next we introduce into Figure 12 also the relationship between d_c and the crystallization temperature, in the form $d_c^{-1}(T_c)$. We know already that the crystal thicknesses measured for the copolymers and the s-PP fall on a common curve. Now we note in addition that this curve gives a straight line in the Gibbs−Thomson plot

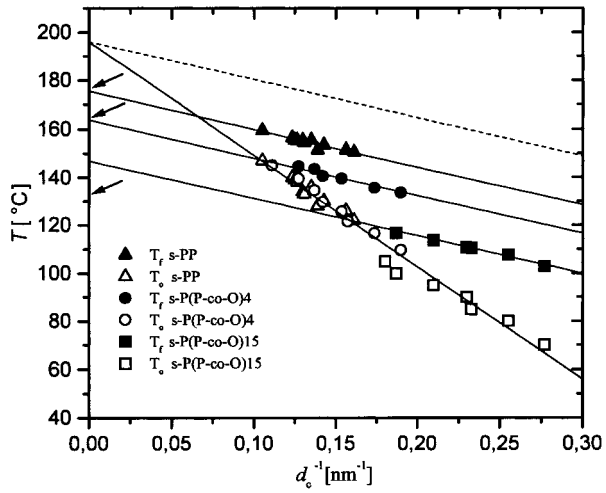

Figure 12. Relations between the inverse crystallite thickness d_c^{-1}, the crystallization temperature T_c and the melting peak T_f, obtained for the two investigated copolymers and the s-PP with 3% meso diads. The dashed line represents the extrapolated $T_f(d_c^{-1})$ dependence of a perfect s-PP. The arrows indicate the zero growth rate-limiting temperatures.

and, as a surprising second important result, it passes with its continuation exactly through the equilibrium melting point of perfect s-PP.

5.3. Conclusions and Some Speculations. The main experimental results as displayed in Figures 4 and 12 may be summarized as follows:

(i) The melting temperatures T_f of the crystallites are located on a series of straight lines with constant slope, with shifts to lower temperatures on increasing x_B. The dependence $T_f(x_B,d_c)$ can therefore be described as

$$T_f(x_B,d_c) = T_f^{\infty,0} - c_1 d_c^{-1} - f(x_B) \tag{11}$$

The function f denotes the x_B dependent shift factor. In the limit of low x_B we find a linear relation

$$f(x_B) = c_2 x_B \tag{12}$$

(ii) The crystallization temperature T_c and the inverse crystal thickness are also linearly related. However, there are no effects from x_B. Hence we may write

$$T_c = T_f^{\infty,0} - c_3 d_c^{-1} \tag{13}$$

or reversely

$$d_c \sim \frac{1}{T_f^{\infty,0} - T_c} \tag{14}$$

The crystal thickness thus obeys a simple law: It is inversely proportional to the supercooling below the equilibrium melting point of perfect s-PP.

(iii) On the other hand, the time required to build up the crystallites greatly varies with x_B. Curves $\tau(T_c)$ have similar shapes; a change in x_B results in a shift along the temperature axis.

A first straightforward conclusion concerns the applicability of the Hoffman−Weeks procedure to determine equilibrium melting points. As demonstrated by Figure 12, it does not work for copolymers and would only be correct for the (nonavailable) perfect homopolymer.

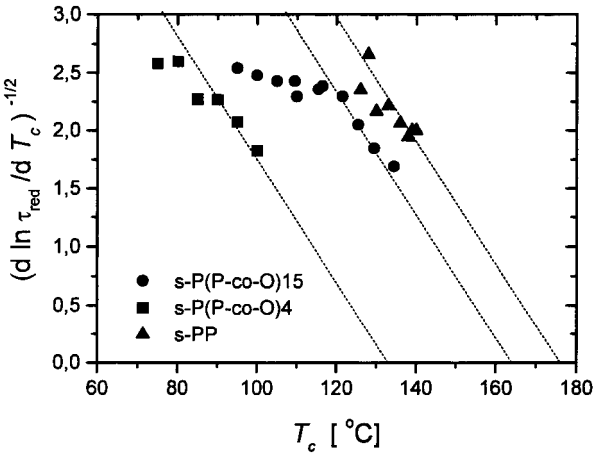

Figure 13. Determination of the zero growth rate temperatures for s-PP and the two copolymers. Plots based on eq 18.

The shape of the curves in Figure 4, showing a steady increase in slope with temperature, suggests for each compound the existence of a limiting temperature with zero growth rate, i.e., infinite τ. For an estimate of these temperatures we started from the familiar relationship (compare for example ref 6, p 162)

$$\tau \sim \exp\frac{T_A}{T_V - T_c} \exp\frac{B_0}{T_c^{\infty}(x_B) - T_c} \tag{15}$$

It explicitly includes the Vogel−Fulcher factor, which accounts for the temperature dependence of the monomeric friction coefficient. The limiting temperature searched for is called $T_c^{\infty}(x_B)$. We introduce the reduced time

$$\tau_{red} = \tau \exp\left[-\frac{T_A}{T_V - T_c}\right] \tag{16}$$

and take the derivative with respect to T_c

$$\frac{d \ln \tau_{red}}{dT_c} = \frac{B_0}{(T_c^{\infty}(x_B) - T_c)^2} \tag{17}$$

Rewriting yields

$$T_c^{\infty}(x_B) - T_c = B_0^{1/2}\left(\frac{d \ln \tau_{red}}{dT}\right)^{-1/2} \tag{18}$$

Figure 13 shows plots according to this relation (choosing $T_A = 700$ K, $T_V = 233$ K, as obtained by viscosity measurements on atactic polypropylene). Surely plots do not allow an accurate determination of the limiting temperatures, but the drawn lines look like a reasonable choice. They imply

$$T_c^{\infty}(x_B) = T_f^{\infty}(x_B) \tag{19}$$

for s-PP and s-P(P-*co*-O)4, but for the copolymer s-P(P-*co*-O)15, since the temperature shifts between the lines in Figure 12 and the curves in Figure 4 are different, we have

$$T_c^{\infty}(x_B) < T_f^{\infty}(x_B) \tag{20}$$

The three arrows in Figure 12 show the locations of T_c^{∞}.

As it appears, the dependence eq 15 does not hold through all temperatures. For s-P(P-*co*-O)4 one observes a break which indicates a change.

The results (i) and (iii) come qualitatively as expected. In agreement with eq 10 we find an additive effect of the finite crystal thickness and the content of noncrystallizable units. A quantitative comparison, however, shows strong deviations from the Flory prediction. Use of eq 1 yields

$$T_f^{\infty,0} - T_f^{\infty}(x_B) = 220\ \text{K}\ x_B$$

whereas the experimental results according to Figure 11 is

$$T_f^{\infty,0} - T_f^{\infty}(x_B) = 716\ \text{K}\ x_B$$

The slope gets smaller at higher values of x_B, and it could be that then it comes more near to the Flory prediction. Deviations toward a stronger effect have been frequently reported (for example, also in ref 3) but so far, there is no convincing explanation. Note that all lines have the same slope, which shows that the surface tension σ_e is not affected by the co-units. The value following from the slope is $\sigma_e = 7.5$ kJ (mol end groups)$^{-1}$ (introducing $\Delta h = 7.7$kJ mol^{-1}[14]).

Absolutely new, for us unexpected, and important is the result (ii): The points $T_c(d_c^{-1})$ of all samples fall on one common curve. Furthermore, in the Gibbs−Thomson plot this curve is a straight line that passes through the equlibrium melting temperature of perfect s-PP. What does this mean? Basically, the line just describes the dependence between the crystal thickness and the crystallization temperature; however, the Gibbs−Thomson form of this relationship suggests that it might represent more, namely again the locus of an equilibrium between crystallites of finite size and the melt. Comparing it with the melting temperature lines $T_f(d_c^{-1})$, we find two important differences: (1) Surface effects are much stronger, as indicated by the about 3 times larger slope. (2) Since we find one common line passing through $T_f^{\infty,0}$ the melt appears as if it would not contain any co-units.

In the first paper dealing with s-PP[4] we used the term native crystals for this initial state. It was proposed that it may differ in both the structure of the surface and interior from the equilibrated crystals melting at T_f and that this reduced perfection could be a consequence of the crystallization kinetics. We also wrote that the properties of the native crystals may change, continuously approaching the equilibrated state when decreasing the growth rate, i.e., increasing the temperature. The new results now partially contradict this view and tell us that the native crystals have a well-defined structure corresponding to a peculiar form with constant properties. We also see that native and final crystal forms differ in the surface structure only. As demonstrated by the limiting behavior $T_c(d_c \rightarrow \infty)$, the heat of melting Δh equals that of perfect s-PP.

The statement in the first paper about the existence of a native crystal form originated from the observation that melting starts already shortly above T_c. For the s-PP sample we found a smooth onset of the melting process. Now, for the copolymers, the melting of the native form shows up even more clearly, with a distinct onset 3 deg above T_c for s-P(P-*co*-O)4 and 5 deg above T_c for s-P(P-*co*-O)15, as indicated by the DSC curves in Figures 9 and 10. The figures prove also that the native crystals indeed change into the relaxed final form. Observations show that the lifetime of the native crystals, i.e., their relative stability, increases with the co-unit content but is finite in principle; for slow enough heating rates one always finds a more or less complete transfer into the relaxed state.

Figure 9 also demonstrates that the building up of the stacks of crystallites, which finally fill the sample, is a sequential process. Obviously, crystals that develop later remain for a longer time in the native phase. The background for this behavior becomes clear when looking in the literature. In electron microscopic studies of the morphology of isothermally crystallized poly(4-methylpentene-1) Bassett and Patel[11] found evidence for the existence of two types of lamellae, dominant ones that grow at first and later form subsidiary lamellae that grow into the intervening space. Both have the same thickness, but they differ in stability, the subsidiary lamellae having lower melting points. Petermann and Gohil reported a similar behavior for isotactic polystyrene.[12] Again melting starts with those crystallites that developed later, filling the remaining space. In our view, all crystals pass through the native form but generally end up with different stabilities due to variations in the efficiency of the perfectioning processes. As it appears, the perfectioning is more difficult for the later grown lamellae. Reasons can be easily envisaged and have already been indicated by these authors. For the inserted crystallites reorganization of the surface region is certainly more complicated, due to the reduced distance of the next neighbor crystals, which affect the environment. In particular, if distances are close, crystals may remain in the native state and then melt immediately above T_c.

Literature also gives hints with regard to a possible cause of the enhanced surface free energy of the native crystallites. In discussions of the primary nucleation of crystals and also the process of crystallization in preoriented melts, i.e., during fiber spinning, some authors assume the occurrence of fringed micelles. Understanding of nucleation rates or melting points based upon this picture then requires us to associate with the basal faces an effective surface free energy that is much larger than that of equilibrated crystallites. The enhancement is due to the crowding of the amorphous cilia at the two surfaces occurring in the absence of a sufficiently high number of sharp folds or close loops. Values for the thus increased surface free energy are given, for example, in Wunderlich's book[13] or in a work of Hoffman,[14] and they amount to several times the normal σ_e. Considering these results, one might think that the surface structure of the native crystallites could have some similarity with fringed micelles. In this context it is interesting to look again in Bassett and Patel's paper. The electron micrograph in Figure 13 presented therein shows localized sites of melting within the subsidiary crystallites, as if individual blocklike crystallites would become unstable and transform into the molten state. Therefore, thinking about the structural properties of the observed transient high surface free energy crystalline form of s-PP, one could envisage a planar arrangement of fringed micelle-like blocks. At present, however, this is just a speculation, as we have no direct evidence for our samples.

There is another puzzling question: Why the melting point of the native crystals remains unaffected by the

presence of the co-units? The osmotic pressure exerted by the co-units looks quenched, but by which mechanism? The behavior is in striking contrast to the melting of the equilibrated crystals, which show an even too strong effect when compared to the Flory prediction. We can only give a first answer. Crystallization results in a demixing of the co-units that are shifted into the amorphous regions. During a subsequent melting they can become effective only under the condition that they are sufficiently mobile to return immediately to the front of the face of melting. The observations on the melting of the native crystals could be understood as indicating that the process of return is hindered. This could be due to the presence of a layer with high entanglement concentration near the crystal surface. Crystal blocks could melt without effecting the entanglement layers and, therefore, without coming in contact with the co-units.

6. The Problems

The experiments on s-PP and the copolymers provided us with clear results and a formally simple scenario, producing a number of questions that are important not only for the understanding of the role of the noncrystallizable units in the crystallization of random copolymers but also for the understanding of polymer crystallization in general. We finish this paper by formulating the main problems:

(i) What is the microscopic structure of the high surface free energy (native) crystal form? We only could offer some speculations, without any proof.

(ii) What is the nature of the relaxation processes that transfer the native crystallites into the final equilibrated form? Exactly these processes are responsible for the stabilization showing up in the difference between the temperatures of crystallization and melting.

(iii) As is evident, measured crystal thicknesses (being unaffected by the presence of noncrystallizable units) and growth rates (being strongly influenced) are independent properties. Which is the rate determining step? Which is the pathway followed in the formation of the native crystals?

Progress in the understanding of polymer crystallization needs answers to these questions.

Acknowledgment. Support of this work by the Deutsche Forschungsgemeinschaft (Graduiertenkolleg Strukturbildung in Makromolekularen Systemen) is gratefully acknowledged. Thanks are also due to the Fonds der Chemischen Industrie for financial help.

References and Notes

(1) Hoffman, J. D.; J. J Weeks. *J. Res. Nat. Bur. Stand., Sect. A* **1962**, *66*, 13.
(2) P. J. Flory. *Principles of Polymer Chemistry*; Cornell University Press: 1953; p 570.
(3) Balbontin, G. Dainelli, D.; Galimberti, M.; G. Paganetto. *Makromol. Chem.* **1992**, *193*, 693.
(4) Schmidtke, J.; Strobl, G.; Thurn-Albrecht, T. *Macromolecules* **1997**, *30*, 5804.
(5) Strobl, G. *Acta Crystallogr.* **1970**, *A26*, 367.
(6) Strobl, G. *The Physics of Polymers*; Springer: Berlin, 1997.
(7) Ruland, W. *Colloid Polym. Sci.* **1977**, *255*, 417.
(8) Thomann, R.; Wang, C.; Kressler, J.; Jüngling, S.; Mülhaupt, R. *Polymer* **1995**, *36*, 3795.
(9) Thomann, R.; Kressler, J.; Mülhaupt, R. *Macromol. Chem. Phys.* **1997**, *198*, 739.
(10) Lovinger, A. J.; Lotz, B.; Davis, D. D.; Padden, F. J., Jr. *Macromolecules* **1993**, *26*, 3494.
(11) Bassett, D. C.; Patel, D. *Polymer* **1994**, *35*, 1855.
(12) Petermann, J.; Gohil, R. M. *Prog.Colloid Polym. Sci.* **1979**, *66*, 41.
(13) Wunderlich, B. *Macromolecular Physics*; Academic Press: New York, 1976; Vol. 2, pp 21, 102.
(14) Hoffman, J. D. *J. Res. Nat. Bur. Stand., Sect. A* **1979**, *83*, 359.

MA980453C